

Photocatalytic performance of titania nanospheres deposited on graphene in coumarin oxidation reaction*

M. WOJTONISZAK[†], B. ZIELINSKA, R. J. KALENCZUK, E. MIJOWSKA

West Pomeranian University of Technology, Szczecin, Institute of Chemical and Environment Engineering,
Pulaskiego 10, 70-322 Szczecin, Poland

In this paper, we present a study on enhanced photocatalytic performance of TiO₂ nanospheres deposited on graphene (n-TiO₂-G) in a process of coumarin oxidation. The enhancement of the photoactivity has been observed in respect to commercial TiO₂ P25. The presented material was prepared in two steps: (i) hydrolysis of titanium (IV) butoxide (TBT) in ethanol solution with simultaneous deposition on graphene oxide (GO) and (ii) calcination of TiO₂-GO to form anatase-TiO₂ and reduce GO to graphene. The nanomaterial was characterized by transmission electron microscopy (TEM), energy dispersive X-ray spectroscopy (EDX), thermogravimetric analysis (TGA), Fourier-Transformed Infrared spectroscopy and Raman spectroscopy. In the presented photocatalytic process the fluorescence was used to detect •OH formed on a photo-illuminated n-TiO₂-G surface using coumarin which readily reacted with •OH to produce highly fluorescent 7-hydroxycoumarin.

Keywords: *graphene, TiO₂, photocatalyst, coumarin*

© Wrocław University of Technology.

1. Introduction

In the past decades, TiO₂ has gained a great interest in photocatalysis area because it is a promising material in many applications connected with air and wastewater purification [1, 2]. Recently, the photocatalytic activity of TiO₂ has been enhanced employing several methods of its modification such as deposition of noble metals [3], fluorination [4], doping [5] and other functionalization processes [6]. One of the methods to improve the photocatalytic performance of TiO₂ is its deposition on graphene. Graphene is a flat monolayer of carbon atoms, tightly packed into a two-dimensional honeycomb lattice [7]. Because of its exceptional properties [8–10] this material has attracted a great interest for potential applications in many fields including electronic devices, fuel cell technology, supercapacitors or nanomedicine [11–13]. As graphene exhibits

high electron mobility, high surface area and high adsorption capacities, it is a promising material for supporting TiO₂ photocatalyst [14]. Furthermore, graphene can improve an efficiency of photo-conversion since it can act as an electron transfer channel and reduce the photo-generated electron holes [15]. So far, several methods have been developed to synthesize TiO₂-graphene nanocomposite [16, 17]. For instance, Guo et al. reported sonochemical preparation of the photocatalyst using TiCl₄ as the substrate of titanium dioxide [18]. They examined the photocatalytic activity of the material in the process of methylene blue degradation and achieved the photocatalyst with higher activity than commercial TiO₂. Wang et al. also stated that TiO₂ nanocrystals deposited on graphene show enhanced photocatalytic activity in the degradation of rhodamine B in comparison to the TiO₂ P25 [19]. Y. Zhang et al. studied the photocatalytic activity of TiO₂ P25/graphene composite, produced in a thermal reaction of graphene oxide, during methylene blue decomposition under visible light irradiation [20]. T. Kamegawa et al. supported TiO₂ on a mesoporous silica surface and the obtained

*This paper was presented at the Conference Functional and Nanostructured Materials, FNMA 11, 6-9 September 2011, Szczecin, Poland

[†]E-mail: mwojtoniszak@zut.edu.pl, Tel: +48 91 449 4772

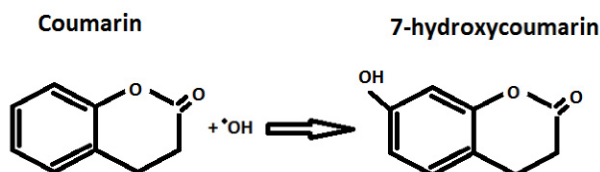


Fig. 1. Formation of 7-hydroxycoumarin by the reaction between coumarin and $\bullet\text{OH}$ radicals.

material coated with graphene [21]. The graphene coating led to enhancement of photocatalytic activity of $\text{TiO}_2/\text{silica}$ for decomposition of 2-propanol in water in comparison to pristine samples. Appropriate adsorption properties of organics favor their transfer to the surface of TiO_2 . The photocatalytic performance of graphene was also examined with other nanocrystals. T. Xu et al. stated that $\text{ZnO}/\text{graphene}$ nanocomposite showed higher photocatalytic activity for the degradation of methylene blue (MB) than pure ZnO [22]. The authors argued that the enhancement of photocatalytic activity of $\text{ZnO}/\text{graphene}$ could be attributed to the high migration efficiency of photo-induced electrons and the inhibited charge carriers recombination due to the electronic interaction between ZnO and graphene.

In the present work, a recently optimized material of titanium dioxide nanospheres adsorbed on graphene in a model reaction of coumarin photooxidation was employed. Coumarin was chosen because it reacts with $\bullet\text{OH}$ radicals to produce 7-hydroxycoumarin which is highly fluorescent. Therefore, this reaction was performed to test photocatalytic activity of $n\text{-TiO}_2\text{-G}$ during these radicals formation. The fluorescence technique was applied to detect $\bullet\text{OH}$. The reaction of coumarin with hydroxyl radical is presented in Fig. 1.

2. Experimental

2.1. Materials

Graphite was purchased from Alfa Aesar. KMnO_4 , sulfuric acid and orthophosphoric acid were obtained from POCH. TBT was

acquired from Aldrich. Ethanol was purchased from Chempur. Coumarin was supplied by Sigma-Aldrich.

2.2. $\text{TiO}_2/\text{graphene}$ preparation

Graphene oxide was synthesized using modified Hummers method [23]. The details on synthesis of TiO_2 nanospheres deposited on graphene are provided elsewhere [24]. Briefly, GO was dispersed in ethanol (1 mg/mL) and a 10 wt.% of TBT ethanol solution was added (GO:TBT = 4:1, vol. ratio). The obtained suspension was ultrasonicated and stirred simultaneously for 90 min. Then, the solution was stirred for 20 h at room temperature. After this step, the mixture was centrifuged (9000 rpm, 1 h), stirred in ethanol for 1 h and centrifuged again (9000 rpm, 1 h) in order to remove the excess of titanium dioxide. Finally, the material was annealed in vacuum ($p = 10^{-7}$ bar) at 400 °C for 2 h to transit the TiO_2 into anatase phase and reduce the graphene oxide to graphene.

2.3. Hydroxyl radical analysis

The formation of hydroxyl radicals ($\bullet\text{OH}$) on the surface of UV illuminated $n\text{-TiO}_2\text{-G}$ was detected by photoluminescence (PL) technique using coumarin. Coumarin reacted with $\bullet\text{OH}$ readily to produce a highly fluorescent product, 7-hydroxycoumarin. Experimental procedure was as follows: 0,3 g of the catalyst was dispersed in 600 cm^3 of 10^{-3} M coumarin aqueous solution. The reaction mixture was mixed for 15 minutes in darkness and then the suspension was exposed to UV light. A medium pressure mercury lamp of 150 W was applied as a light source. The lamp provided light of the wavelength ranging from 200 to 600 nm with the maximum intensity of 366 nm. The fluorescence emission spectrum (excited at 332 nm) of the coumarin solution was measured every 5 min of illumination. The fluorescence spectra were recorded on F-7000 Fluorescence spectrometer (Hitachi). The photocatalytic activity of $n\text{-TiO}_2\text{-G}$ was compared to the commercial TiO_2 P25. The dosage of TiO_2 P25 containing the same amount of Ti loading such as in $n\text{-TiO}_2\text{-G}$ have been used.

2.4. Characterization

The morphology and chemical composition of the sample was examined using high resolution transmission electron microscopy (TEM, Tecnai F30) and the energy dispersive X-ray (EDX) spectroscopy. Thermal stability of the materials was investigated using SDT Q600 Simultaneous TGA/DSC under air flow (100 mL/min) and at the heating rate of 10 °C/min. FT-IR absorption spectra were recorded on Nicolet 6700 FT-IR Spectrometer. The samples were prepared in KBr tablets. Briefly, ~0,5 mg of each measured sample was mixed in a mortar with about 400 mg of KBr and next pressed in a hydraulic press to form a stable tablet. Raman spectra were recorded using Via Raman Microscope (Renishaw), with the excitation wavelength of 514 nm.

3. Results and discussion

The n-TiO₂-G photocatalyst was produced in the hydrolysis process of TBT in ethanol solution in the presence of graphene oxide followed by calcination. The calcination step was performed in order to form the anatase phase of titanium dioxide and to remove oxygen-containing functional groups from the graphene oxide. In this process the anatase-TiO₂ was deposited on graphene surface. The morphology and composition of the material was characterized using transmission electron microscopy with energy dispersive X-ray spectroscopy as its mode. Fig. 2A and 2B present TEM images of the photocatalyst. On the basis of detailed TEM analysis, the distribution of the diameters was determined and the results are presented in the Fig. 2C. According to the study it was observed that the nanospheres with diameters ranging from 100 nm to 250 nm were deposited on the graphene. It was found that the dominating fraction contains titania nanospheres with a diameter between 176 nm and 200 nm.

Fig. 3 presents the EDX spectrum of the prepared photocatalyst. The analysis did not detect any elements other than Ti, O, C (Cu from TEM grid), which fully confirms the composition of titanium dioxide adsorbed on graphene.

In order to perform a quantitative analysis of the photocatalyst the TGA was applied. The samples were heated under air flow with the heating rate of 10 °C/min. The TGA curves of GO and n-TiO₂-G are presented in Fig. 4. Graphene oxide exhibits mass loss between 150 °C and 300 °C which is related to the removal of oxygen-containing functional groups. A significant mass loss was observed at the temperature range between 450 and 600 °C for both GO and n-TiO₂-G. This happened due to the pyrolysis of carbon skeleton [25]. In the TGA curve of n-TiO₂-G there is no mass loss at the temperature range between 150 °C and 300 °C, which confirms a successful reduction of GO into graphene during the calcination. The weight loss of n-TiO₂-G was stabilized at approximately 95 wt.% at the temperatures between 700 °C and 800 °C indicating that the amount of graphene used as titania support was about 5 wt.%.

For further characterization, FT-IR spectroscopy was used and the obtained spectra of GO and n-TiO₂-G are presented in Fig. 5. Graphene oxide depicts strong C-O absorption peaks at 1010 cm⁻¹, 1070 cm⁻¹, 1170 cm⁻¹ and 1270 cm⁻¹ attributed to alkoxy, epoxy and carboxyl groups. C=O stretching vibration peak from carboxyl group is observed at approximately 1720 cm⁻¹. The absorption peaks at 1640 cm⁻¹ and at 3450 cm⁻¹ detected in each spectrum, are attributed to C=C aromatic bond and O-H vibration, respectively [26]. In the n-TiO₂-G spectrum the peak related to the oxygen-containing functional groups disappeared suggesting a complete reduction of GO during the calcination. In this spectrum strong peaks at 620 cm⁻¹, 655 cm⁻¹ and 678 cm⁻¹ related to Ti-O-Ti bond are observed [18, 27]. This fully confirms the hydrolysis of titanium butoxide and the formation of TiO₂. Furthermore, a peak at 1130 cm⁻¹ is ascribed to the vibration of Ti-O-C bond indicating that titania nanospheres are chemically bounded with graphene [28, 29].

To determine the crystal phase of the obtained photocatalyst Raman spectroscopy was used. The measurement was performed using an excitation laser with a wavelength of 514 nm. According

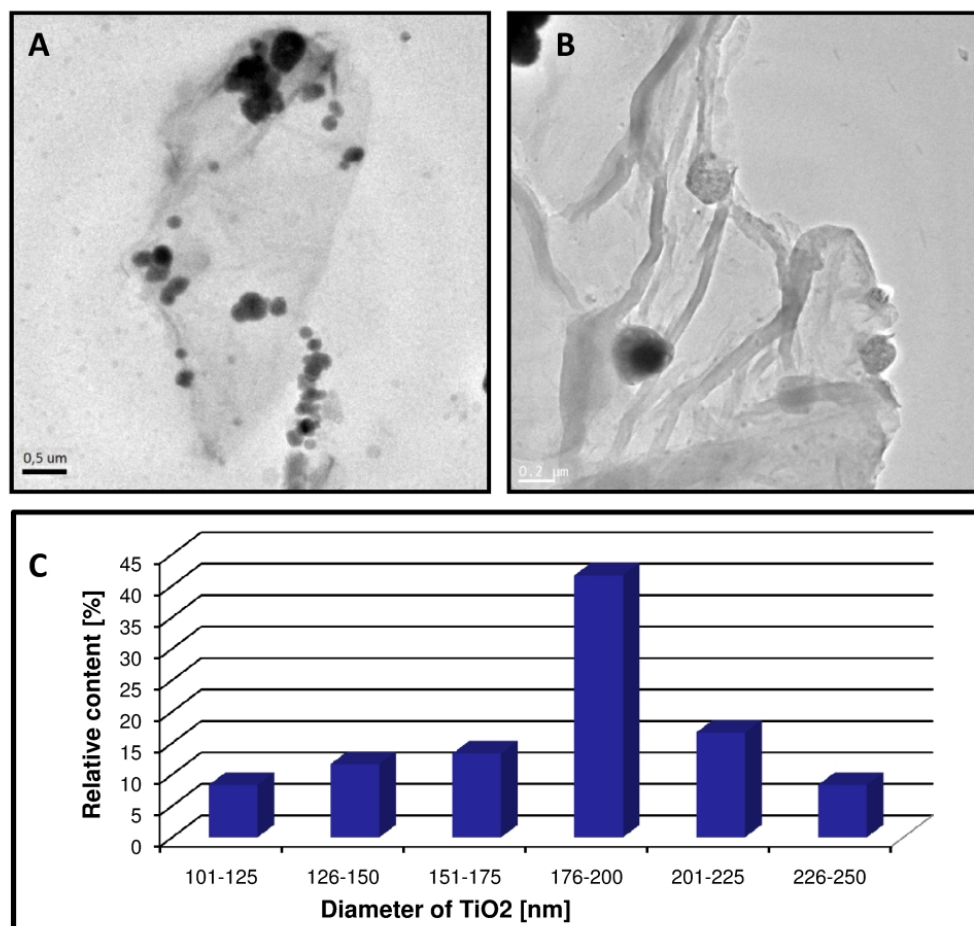


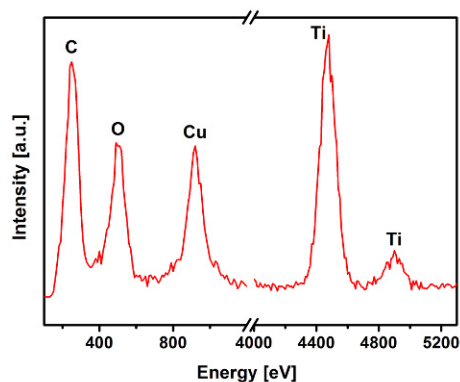
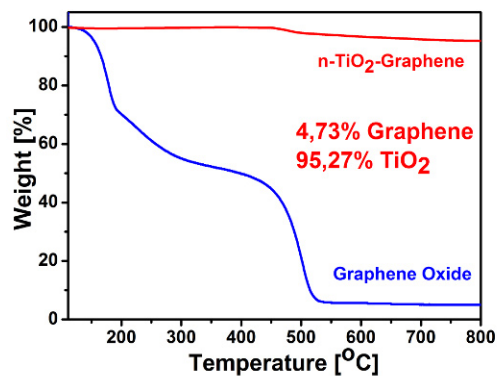
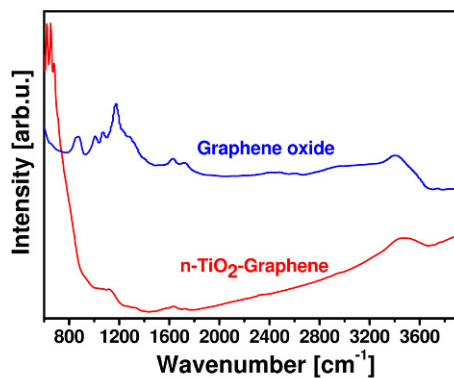
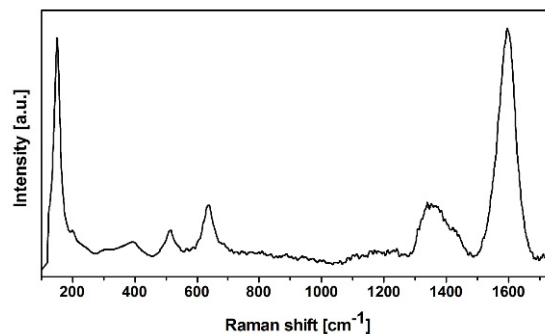
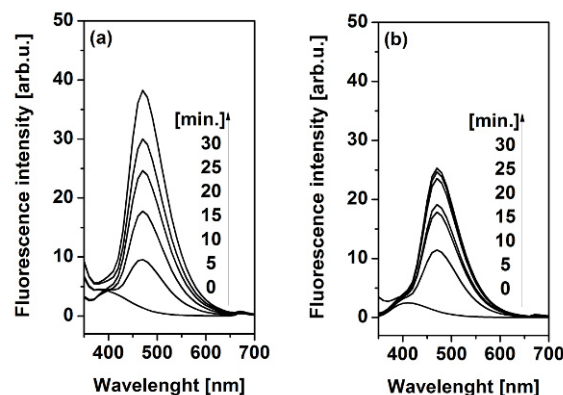
Fig. 2. TEM images of n-TiO₂-G (A, B) and the distribution of the diameters of TiO₂ nanospheres (C).

to Ohsaka [30], the Raman spectrum of anatase crystal exhibits six modes at the following positions: 144 cm⁻¹ (E_g), 197 cm⁻¹ (E_g), 399 cm⁻¹ (B_{1g}), 513 cm⁻¹ (A_{1g}), 519 cm⁻¹ (B_{1g}), and 639 cm⁻¹ (E_g). In Fig. 6 the Raman spectrum of n-TiO₂-graphene is presented. It is clearly seen that this spectrum consists of all modes characteristic of anatase. In addition, the modes corresponding to graphene are present at 1358 cm⁻¹ and 1596 cm⁻¹. The first – D band – is a breathing mode of A_{1g} symmetry in carbon lattice. The second – G band – originates from the in-plane vibration of sp² carbon atoms (E_{2g} symmetry) [31].

The changes of fluorescence emission spectra for the coumarin solution, excited at 332 nm in the presence of n-TiO₂-G and TiO₂ P25, with

irradiation time are shown in Figs. 7a and 7b, respectively. It can be clearly seen that a gradual increase in the fluorescence intensity at ~460 nm is observed with increasing the irradiation time. It is known that the fluorescence at ~460 nm is characteristic of 7-hydroxycoumarin [32]. This confirms that fluorescent 7-hydroxycoumarin was formed during the photocatalytic reaction on n-TiO₂-graphene and TiO₂ P25 due to the reaction between •OH and coumarin (see Fig. 7).

Fig. 8 shows the plots of fluorescence intensity at 460 nm versus irradiation time. The linear increase of the fluorescence intensity up to 30 min of UV illumination has been observed. This phenomenon is a result of •OH radicals generation on the n-TiO₂-G and TiO₂ P25 surface,

Fig. 3. EDX spectrum of n-TiO₂-G.Fig. 4. TGA curves of graphene oxide and n-TiO₂-G.Fig. 5. FT-IR spectra of graphene oxide and n-TiO₂-G.Fig. 6. Raman spectrum of n-TiO₂-G photocatalyst.Fig. 7. Fluorescence spectral changes during illumination of n-TiO₂-G (a) and TiO₂ P25 (b) in aqueous solution of coumarin (excitation at 332 nm).

which is proportional to the irradiation time and therefore, described by zero-order kinetics [33]. Moreover, the formation rate of •OH on the n-TiO₂-graphene is much larger than that of TiO₂ P25. Recently, Q. Xiang et al. reported that the formation rate of •OH on the surface of irradiated commercial P25 was much higher than that of other semiconductors [32]. In this paper we present an enhanced photocatalytic activity of anatase-TiO₂ nanospheres adsorbed on graphene in comparison to the commercial ones. The higher activity may be due to chemical bonding between TiO₂ and graphene. Because graphene exhibits excellent electronic transport properties, it favors a better separation of the photogenerated electron-hole pairs and prevents their recombination.

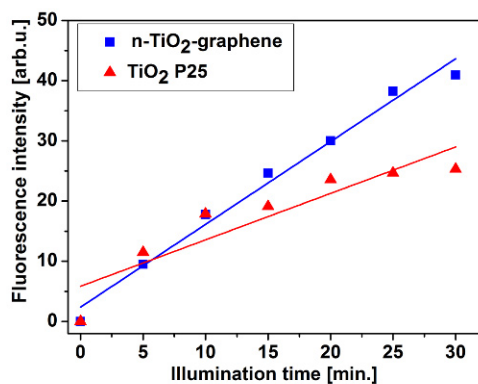


Fig. 8. Plots of the induced fluorescence intensity at 460 nm versus irradiation time for coumarin on TiO₂ P25 and n-TiO₂-graphene photocatalysts.

4. Conclusions

We presented characterization and photocatalytic activity of TiO₂ nanospheres deposited on graphene in a model reaction of coumarin oxidation. The material was synthesized in a facile TBT hydrolysis in ethanol solution with simultaneous deposition on GO followed by calcination of TiO₂-GO to form anatase-TiO₂ and reduce GO to graphene. The prepared photocatalyst was composed of graphene (5 wt.%) chemically bonded with TiO₂ nanospheres and exhibited an enhanced photocatalytic activity in comparison to the commercial TiO₂ P25. The high photoactivity of n-TiO₂-graphene can be explained by the remarkable electronic transport properties which favor better separation of the photogenerated electron-hole pairs and prevent their recombination. Hence, the material is a promising photocatalyst in different photocatalytic reactions which are currently under investigations.

Acknowledgements

The authors are grateful for the financial support of Foundation for Polish Science within FOCUS 2010 Program.

References

[1] TARANTO J., FROCHOT D., PICHAT P., *Sep. Pur. Techn.*, 67 (2009), 187.
 [2] PEKAKIS P.A., XEKOUKOULOTAKIS N.P.,

MANTZAVINOS D., *Wat. Res.*, 40 (2006), 1276.
 [3] SUBRAMANIAN V.E., WOLF E., KAMAT P.V., *J. Am. Chem. Soc.*, 126 (2004), 4943.
 [4] HWAJIN K., WONYONG C., *Appl. Cat. B: Environ.*, 69 (2007), 127.
 [5] KAMAT P.V., *Pure Appl. Chem.*, 74 (2002), 1693.
 [6] HUANG J., WANG X., HOU Y., CHEN X., WU L., WANG X., FU X., *Microporous and Mesoporous Mat.*, 110 (2008), 543.
 [7] GEIM A.K., NOVOSELOV K.S., *Nat. Mat.*, 6 (2007), 183.
 [8] LI X.L., WANG X.R., ZHANG L., LEE S.W., DAI H.J., *Science*, 319 (2008), 1229.
 [9] BALANDIN A.A. et al., *Nano Lett.*, 8 (2008), 902.
 [10] LEE C., WEI X.D., KY SAR J.W., HONE J., *Science*, 321 (2008), 385.
 [11] WANG X., ZHI L.J., MULLEN K., *Nano Lett.* 8, 323 (2008).
 [12] CHEN S., ZHU J., WU X., HAN Q., WANG X., *Acs Nano*, 4 (2010), 2822.
 [13] CHANG Y. et al., *Toxicol. Lett.*, 200 (2011), 201.
 [14] YOO D.H. et al., *Curr. Appl. Phys.*, 11 (2011), 805.
 [15] ZHANG X.Y., LI H.P., CUI X.L., *Chin. J. Inorg. Chem.*, 25 (2009), 1903.
 [16] WANG Y., SHI R., LIN J., ZHU Y., *Appl. Cat. B: Environ.*, 100 (2010), 179.
 [17] ZHANG H., LV X., LI Y., WANG Y., LI J., *Acs Nano*, 4 (2010), 380.
 [18] GUO J., ZHU S., CHEN Z., LI Y., YU Z., LIU Q., LI J., FENG C., ZHANG D., *Ultrason. Sonochem.*, 18 (2011), 1082.
 [19] WANG F., ZHANG K., *J. Mol. Cat. A: Chem.*, 345 (2011), 101.
 [20] ZHANG Y., PAN CH., *J. Mater. Sci.*, 46 (2011), 2622.
 [21] KAMEGAWA T., YAMAHANA D., YAMASHITA H., *J. Phys. Chem. C*, 114 (2010), 15049.
 [22] XU T., ZHANG L., CHENG H., ZHU Y., *Appl. Catal. B.*, 101 (2011), 382.
 [23] MARCANO D.C. et al., *Acs Nano*, 4 (2010), 4806.
 [24] WOJTONISZAK M., ZIELINSKA B., CHEN X., KALENCZUK R.J., BOROWIAK-PALEN E., *J. Mater. Sci.*, 47 (2012), 3185.
 [25] JEONG H.K., LEE Y.P., JIN M.H., KIM E.S., BAE J.J., LEE Y.H., *Chem. Phys. Lett.*, 470 (2009), 258.
 [26] LAZAR G., ZELLAMAA K., VASCAN I., STAMATE M., LAZAR I., RUSU I., *J. Optoelectr. and Adv. Mat.*, 7 (2005), 647.
 [27] WANG G., WANG B., PARK J., YANG J., SHEN X., YAO J., *Carbon*, 47 (2009), 68.
 [28] KUMAR P.M., BADRINARAYANAN S., SASTRY M., *Thin Solid Films*, 358 (2000), 122.
 [29] MEROUANI A., AMARDIJA-ADNANI H., *International Scientific Journal for Alternative Energy and Ecology*, 6 (2008), 151.
 [30] OHSAKA T., *J. Phys. Soc. Jpn.*, 48 (1980), 1661.
 [31] FERRARI A.C., ROBERTSON J., *Phys. Rev. B*, 61 (2000), 14095.

- [32] XIANG Q., YU J., WONG P.K., *J. Colloid Interf. Sci.*, 357 (2011), 163.
- [33] ISHIBASHI K., FUJISHIMA A., WATANABE T., HASHIMOTO K., *Electrochem. Commun.*, 2 (2000), 207.

Received 2012-03-09

Accepted 2012-05-07